

# Jahn-Teller Coupled Charge Density Wave in A Two Orbital Double Exchange System

M anidipa Mitra

S.N. Bose National Centre for Basic Sciences, JD Block,  
Sector III, Salt Lake City, Kolkata - 700 098, India

PACS No. 63.20.-e, 71.45.Lr, 71.20.Bc, 75.47.Lx.

## Abstract

In a two orbital double exchange model we formulate Jahn-Teller coupled charge density wave in half-filled limit. Softening of Jahn-Teller phonons corresponding to distortion modes  $Q_2$  or  $Q_3$  associated with perfect nesting of Fermi surface leads to this instability at low temperature. The gap equation for charge density wave state and its dependences on electron-lattice coupling are calculated explicitly when any one of the Jahn-Teller modes is excited cooperatively. We find that the  $Q_2$  distortion mode yields lowest free energy. The calculated heat capacity for each mode shows  $T^3$  behavior at low temperature. Effect of electron-lattice interaction on collective mode, such as amplitude mode, is more pronounced when the excited mode is  $Q_2$ .

## 1. Introduction

It is widely accepted that the collective nature of coupling of  $e_g$  electrons to the underlying lattice degrees of freedom have great impact on extraordinary properties of the colossal magnetoresistive (CMR) manganites [1]. The parent compound LaMnO<sub>3</sub> contains Jahn-Teller (JT) ions Mn<sup>3+</sup>, which is orbitally degenerate. The on-site vibrational modes of the MnO<sub>6</sub> octahedra are breathing mode Q<sub>1</sub> and the Jahn-Teller modes { Q<sub>2</sub> (in-plane distortion mode), Q<sub>3</sub> (octahedral stretching mode) }. Due to the coupling between the  $e_g$  electrons and Q<sub>2</sub>, Q<sub>3</sub> modes the degeneracy of Mn<sup>3+</sup> is lifted. In the lattice the MnO<sub>6</sub> octahedra are co-operatively stretched out, resulting a C - type orbital and A - type spin antiferromagnetic structure [2]. Several recent experimental investigations such as high-resolution electron microscopy [3], THz time-domain spectroscopy [4], high-resolution ARPES [5], non-linear electrical response [6], X-ray and neutron scattering [7,8] measurements reveal the evidence of charge density waves in different composition of CMR manganites. Moreover, ARPES results [5] show Fermi surface nesting, which ensures the possibility of density wave formation in these materials. It is well known that in a low dimensional one orbital system, due to particular geometry of the Fermi surface, electron-phonon interactions lead to periodic lattice distortions. This results a ground state characterized by a gap in the single particle excitation spectrum at low temperature, which is known as charge density wave (CDW) [9]. In CMR manganites the Jahn-Teller vibrational modes play a major role to shape the properties of these systems compared to the breathing mode phonon Q<sub>1</sub> which does not alter the symmetry of the MnO<sub>6</sub> octahedron. The distribution of charge density at two  $e_g$  orbitals,  $d_{x^2-y^2}$  and  $d_{3z^2-r^2}$ , depends on excited JT mode. In presence of these two orbitals, the electron can be either in any one of the orbitals or in any linear combination of two [10]. It appears that the perfect nesting of the Fermi surface associated with Jahn-Teller distortions may give rise to possibilities of occurrence of charge density waves in these systems. Therefore, the

resulting charge density wave will be coupled to the orbital order of the system. We denote this density wave as Jahn-Teller coupled charge density wave (JT CCDW).

In the present work, we investigate the formation of Jahn-Teller coupled charge density wave instability in two orbital, double exchange model with one electron per site. The paper is organized as follows. In section 2 we formulate the Hamiltonian for Jahn-Teller coupled charge density wave in two dimension and calculate the JT CCDW order parameter for different JT vibrational modes. To determine the dominant JT distortion mode, we calculate the free energy and hence heat capacity in the JT CCDW state. In the same spirit of CDW system, the spectral density functions of the ordered ground state are calculated from the amplitude mode response function of JT CCDW state generated due to each JT active mode. The results of our calculations are presented in section 3. Lastly, in section 4 we make some concluding remarks.

## 2. Formalism

We consider two orbital double exchange model in two dimension, and large Hund's rule coupling limit in which the ground state configuration corresponds to the itinerant spin being parallel to the core spin at each site. If one compares our model with the manganite (e.g. LaMnO<sub>3</sub>) system the core spins and the itinerant electrons may be identified with the t<sub>2g</sub><sup>3</sup> (localized) electrons and the e<sub>g</sub><sup>1</sup> (mobile) electrons of Mn<sup>3+</sup> ion respectively. We take the value of core spin at each site as S =  $\frac{3}{2}$ . The kinetic part of the Hamiltonian in momentum representation is given by

$$H_1 = \sum_k B_k^Y T B_k; \quad (1)$$

where  $B_k^Y = (d_{1,k}^Y; d_{2,k}^Y)$  with  $d_1$  and  $d_2$  being the e<sub>g</sub>-electron annihilation operators in two orthonormal orbitals  $d_{x^2-y^2}$  and  $d_{3z^2-r^2}$  respectively. The elements of the hopping matrix T are given by  $T_{1,1} = -1.5\epsilon[\cos k_x + \cos k_y]$ ,  $T_{2,2} = -0.5\epsilon[\cos k_x + \cos k_y]$ , and  $T_{1,2} = 0.5\epsilon[\cos k_x - \cos k_y]$ . The transfer hopping integral t is modified as  $t = t \cos(\frac{\pi}{2})$  because of double exchange interaction [11]. We take the average value

of the parameter  $\cos(\frac{\pi}{2}) = \frac{S_0 + \frac{1}{2}}{2S+1}$ , where  $S_0 = \frac{7}{2}$ , and  $\frac{1}{2}$  for ferromagnetic (FM) and antiferromagnetic (AFM) spin arrangements respectively.  $S = \frac{3}{2}$  is the magnitude of localized  $t_{2g}$  spin at each site. This results  $\tau = t$  for FM and  $0.25t$  for AFM spin ordering. So the spin degrees of freedom may be omitted in the Hamiltonian without loss of generality.

The Jahn-Teller coupling parts of the Hamiltonian for  $Q_2$  and  $Q_3$  mode can be written as [10]

$$H_{Q_2} = g \sum_i^X Q_{2i} (d_{1i}^y d_{2i} + d_{2i}^y d_{1i}); \quad (2)$$

$$H_{Q_3} = g \sum_i^X Q_{3i} (d_{1i}^y d_{1i} - d_{2i}^y d_{2i}); \quad (3)$$

where  $g$  is the electron-JT phonon coupling strength. To diagonalize the kinetic part of the Hamiltonian appearing in equation (1) we introduce the new fermionic operators  $c_k^1$  and  $c_k^2$  as

$$\begin{aligned} c_k^1 &= \sin \frac{k}{2} d_{1,k} + \cos \frac{k}{2} d_{2,k}; \\ c_k^2 &= \cos \frac{k}{2} d_{1,k} - \sin \frac{k}{2} d_{2,k}; \end{aligned} \quad (4)$$

with  $\tan k = \frac{\sqrt{3}(\cos k_x \cos k_y)}{(\cos k_x + \cos k_y)}$ . The eigen values of the kinetic energy are given by  $E_{n,k} = \sqrt{\cos^2 k_x + \cos^2 k_y - \cos k_x \cos k_y}$  where  $n = 1, 2$ . The Fermi sea corresponding to  $k_{1,k}$  is the intersection of the region  $k_x = \pm \frac{\pi}{2}$  with the region  $k_y = \pm \frac{\pi}{2}$  and corresponding to  $k_{2,k}$  is the union of the region  $k_x = \pm \frac{\pi}{2}$  with all values of  $k_y$  allowed) to the region  $k_y = \pm \frac{\pi}{2}$  (with all values of  $k_x$  allowed). It is evident from the symmetry of the bands that at half-filling  $k_{1(2),k} = \pm \frac{\pi}{2(1+\sqrt{3})}$  for  $Q = (0, 0)$ , which shows a perfect nesting at wave vector  $Q$ .

The lattice instability in low dimensional system is usually driven by the softening of the wave vector  $Q$  due to electron-phonon (e-ph) interactions, which is called Kohn anomaly. This is a precursor to the Peierls transition. Peierls instability brings

about the formation of the CDW with an accompanying periodic lattice distortion which in turn gives rise to a band gap at the Fermi level driving the system from a conductor to an insulator. In order to find how the JT phonon  $Q_2$  or  $Q_3$  softens to set similar instability, it is needed to calculate the phonon self-energy arising from e-ph interaction for  $Q_2$  or  $Q_3$  mode. The phonon response function is determined by the phonon Green's function given by [12],

$$D_{q;q^0}(q; q^0; !) = \frac{!_q - q;q^0}{!_q^2 - !_q(q; q^0; !)} \quad (5)$$

Here  $(q; !)$  is the self-energy acquired by the  $q$ -th phonon and  $!_q$  is the bare phonon frequency. The phonon self-energy is given by

$$(\mathbf{q}; !) = 4\pi^2 g^2 \rho(\mathbf{q}; !); \quad (6)$$

where  $\rho(\mathbf{q}; !)$  is the density response function. We denote  $(q; !)$  as  $\rho_2(q; !)$  and  $\rho_3(q; !)$  respectively for  $Q_2$  and  $Q_3$  distorted modes.

The phonon response function for  $Q_2$  and  $Q_3$  mode can be written as [13],

$$\begin{aligned} \rho_2(q; !) &= \sum_k \frac{h\hbar \rho_2(q) \rho_2(q) \text{ii}_k}{\omega_k^2 - \omega_2(q) \text{ii}_k}; \\ \rho_3(q; !) &= \sum_k \frac{h\hbar \rho_3(q) \rho_3(q) \text{ii}_k}{\omega_k^2 - \omega_3(q) \text{ii}_k}; \end{aligned} \quad (7)$$

where  $\rho_2(q) = (d_{1,k+q}^y d_{2k} + d_{2,k+q}^y d_{1k})$  and  $\rho_3(q) = (d_{1,k+q}^y d_{1k} - d_{2,k+q}^y d_{2k})$ . The renormalized phonon frequency with the wave vector  $q = jQ$  corresponding to the  $Q_2$  or  $Q_3$  mode can be determined from the pole of the phonon Green's function, with the static response functions  $\rho_2(Q; 0)$  or  $\rho_3(Q; 0)$  respectively. It can be shown [14] that  $\rho_2(Q; 0)$  and  $\rho_3(Q; 0)$  diverges at  $T \rightarrow 0$ .

The response function  $\rho_2(Q; 0)$  diverges faster than  $\rho_3(Q; 0)$  [14]. The divergence of the response functions with decreasing temperature indicate the softening of  $Q_2$  and  $Q_3$  vibrational modes and hence a possibility of Fermi surface instability. The temperature at which the soft mode frequency for  $Q_2$  or  $Q_3$  vanishes is the Jahn-Teller coupled charge density wave transition temperature  $T_{CDW}$ .

In this report, we formulate the Jahn-Teller coupled charge density wave when either  $Q_2$  or  $Q_3$  mode gets excited cooperatively. For this purpose we use the transformation (4) and second quantized form of the phonon modes given by  $(b_q^{2(3)} + b_q^{2(3)*})$  for the wave vector  $q = Q$  in equations (2) and (3). By using canonical transformation [15], we derive the effective electron-electron interaction mediated by e-ph interaction as,

$$H_{Q_2}^{e-e} = \sum_{kk^0}^X jg_{kk^0} j \sin_{k^0} (c_{k^0+Q}^{1y} c_{k^0}^2 + c_{k^0}^{2y} c_{k^0+Q}^{1y} + c_{k^0}^{1y} c_{k^0+Q}^2 + c_{k^0+Q}^{2y} c_{k^0}^{1y}) \\ \sin_k (c_{k+Q}^{1y} c_k^2 + c_k^{2y} c_{k+Q}^{1y} + c_k^{1y} c_{k+Q}^2 + c_{k+Q}^{2y} c_k^{1y}); \quad (8)$$

$$H_{Q_3}^{e-e} = \sum_{kk^0}^X jg_{kk^0} j \cos_{k^0} (c_{k^0+Q}^{1y} c_{k^0}^2 + c_{k^0}^{2y} c_{k^0+Q}^{1y} + c_{k^0}^{1y} c_{k^0+Q}^2 + c_{k^0+Q}^{2y} c_{k^0}^{1y}) \\ \cos_k (c_{k+Q}^{1y} c_k^2 + c_k^{2y} c_{k+Q}^{1y} + c_k^{1y} c_{k+Q}^2 + c_{k+Q}^{2y} c_k^{1y}); \quad (9)$$

where  $g_{kk^0}$  is considered as average interaction strength and  $g_{kk^0} = jg_{kk^0} j$ . It is to be mentioned here, while deriving the equations (8), (9) we have considered only terms like  $c^{1(2)y} c^{2(1)}$  in the electron-phonon interaction.

Now we write the total Hamiltonian corresponding to  $Q_2$  and  $Q_3$  as,

$$H^{Q_2(Q_3)} = H_1 + H_{e-e}^{Q_2(Q_3)}; \quad (10)$$

In the mean-field approximation, the JT CCDW order parameter ( $\chi$ ) for  $Q_2$  and  $Q_3$  modes are respectively defined as,

$$\chi_2 = \frac{1}{2} (\sin_k) = \sum_{k^0}^X jg_{kk^0} j \sin_{k^0} \sin_k \\ hc_{k^0+Q}^{1y} c_{k^0}^2 + c_{k^0}^{2y} c_{k^0+Q}^{1y} + c_{k^0}^{1y} c_{k^0+Q}^2 + c_{k^0+Q}^{2y} c_{k^0}^{1y}; \quad (11)$$

$$\chi_3 = \frac{1}{3} \cos_k = \sum_{k^0}^X jg_{kk^0} j \cos_{k^0} \cos_k \\ hc_{k^0+Q}^{1y} c_{k^0}^2 + c_{k^0}^{2y} c_{k^0+Q}^{1y} + c_{k^0}^{1y} c_{k^0+Q}^2 + c_{k^0+Q}^{2y} c_{k^0}^{1y}; \quad (12)$$

where  $\chi_2$  ( $\chi_3$ ) is the amplitude of the JT CCDW gap generated due to  $Q_2$  ( $Q_3$ ) mode. Therefore, the JT CCDW Hamiltonian can be obtained from (10) as

$$H_{JTCCDW}^{Q_2(Q_3)} = \sum_k \left[ c_{1,k}^{1y} c_{1,k}^1 + c_{1,k+Q}^{2y} c_{1,k+Q}^2 \right] + \sum_k \left[ c_{2,k}^{2y} c_{2,k}^2 + c_{2,k+Q}^{1y} c_{2,k+Q}^1 \right] + \sum_k \left[ c_{1,k+Q}^{1y} c_{1,k}^2 + c_{1,k}^{2y} c_{1,k+Q}^1 + c_{2,k+Q}^{1y} c_{2,k}^2 + c_{2,k}^{2y} c_{2,k+Q}^1 \right]; \quad (13)$$

while  $c_k$  is different for  $Q_2$  and  $Q_3$  mode according to equations (11) and (12).

To diagonalize the Hamiltonian  $H_{JTCCDW}^{Q_2(Q_3)}$  we use the following two simultaneous canonical transformations :

$$\begin{aligned} c_{1,k} &= \sin \frac{k}{2} c_k^1 + \cos \frac{k}{2} c_{k+Q}^2; \\ c_{1,k} &= \cos \frac{k}{2} c_k^1 - \sin \frac{k}{2} c_{k+Q}^2; \end{aligned} \quad (14)$$

where  $\cos(\frac{k}{2}) = \frac{1}{2} (1 - p \frac{1}{2})^{\frac{1}{2}}$ ,  $\sin(\frac{k}{2}) = \frac{1}{2} (1 + p \frac{1}{2})^{\frac{1}{2}}$  and

$$\begin{aligned} c_{2,k} &= \sin \frac{k}{2} c_k^2 + \cos \frac{k}{2} c_{k+Q}^1; \\ c_{2,k} &= \cos \frac{k}{2} c_k^2 - \sin \frac{k}{2} c_{k+Q}^1; \end{aligned} \quad (15)$$

with  $\cos(\frac{k}{2}) = \frac{1}{2} (1 - p \frac{2}{2})^{\frac{1}{2}}$  and  $\sin(\frac{k}{2}) = \frac{1}{2} (1 + p \frac{2}{2})^{\frac{1}{2}}$ . These transformations yield the quasi particle energies as  $E_k^1 = E_k^1 = \frac{1}{(\frac{2}{1,k} + \frac{2}{k})}$  and  $E_k^2 = E_k^2 = \frac{1}{(\frac{2}{2,k} + \frac{2}{k})}$ , which correspond to resulting four bands  $1, 1, 2$  and  $2$  respectively. The diagonalized Hamiltonian in presence of either  $Q_2$  or  $Q_3$  mode can now be written as,

$$H_{JTCCDW}^{Q_2(Q_3)} = \sum_k \left[ E_k^1 \left( \begin{array}{cc} 1 & 1 \\ 1 & 1 \end{array} \right) + E_k^2 \left( \begin{array}{cc} 1 & 1 \\ 1 & 1 \end{array} \right) \right]; \quad (16)$$

The gap equations can be written for  $Q_2$  mode as

$$1 = g \sum_k \sin^2 \left[ \frac{\tanh(E_k^1=2)}{E_k^1} + \frac{\tanh(E_k^2=2)}{E_k^2} \right]^{\frac{1}{2}}; \quad (17)$$

and for the  $Q_3$  mode as

$$1 = g \sum_k \cos^2 \left[ \frac{\tanh(E_k^1=2)}{E_k^1} + \frac{\tanh(E_k^2=2)}{E_k^2} \right]^{\frac{1}{2}}; \quad (18)$$

where for simplicity we have taken  $g_{kk0} \neq g$ . It is clear that both the amplitudes  $2$  and  $3$  are symmetric in  $k_x$  and  $k_y$  sector of the Fermi surface, but  $k$  are highly

anisotropic in  $k$ -space. The effective temperature,  $T^* = k_B T t$  enters in (17) and (18) through  $\beta = 1/(k_B T t)$ . The free energy of the system can then be calculated as

$$F = -\frac{1}{k_B T} \sum_{\mathbf{k}} \ln(1 + e^{-E_{\mathbf{k}}^*}); \quad (19)$$

where  $E_{\mathbf{k}}^* = E_{\mathbf{k}}^{1,1}, E_{\mathbf{k}}^{1,2}, E_{\mathbf{k}}^{2,1}, E_{\mathbf{k}}^{2,2}$ . Hence the heat capacity can also be calculated from the relation,

$$C_V = T \frac{d^2 F}{dT^2}; \quad (20)$$

We like to point out here that the four band Hamiltonian, similar to equation (16), is also obtained by Jackeli et al [16] considering only nearest neighbor Coulomb correlation in a double degenerate system. To explain the nontrivial observed order in  $\text{LaMnO}_3$ , several studies have been reported based on either purely Coulombic interaction or Jahn-Teller interaction [1]. In the framework of two orbital model, purely Coulombic approaches produce correct spin ordered (A-type spin antiferromagnetic) state [17,18], while giving conflicting results regarding the orbital order that co-exists with the A-type spin state. According to Hotta et al [19], Jahn-Teller based calculations lead to experimentally observed A-type spin and C-type orbital order in a model for undoped manganites. Therefore, in the present calculation focussing on undoped manganites, we formulate our model based on the Jahn-Teller coupling.

The robustness of the ordered ground state is usually tested by looking at the response of the system to small fluctuations. In case of CDW state, it is well known that fluctuations of the phase and the amplitude of the order parameter results in the appearance of the collective modes of the system [9]. The amplitude mode is a measure of the CDW order parameter. In the present work, we want to calculate the spectral density function for the JTCCDW state, from the amplitude response function  $\tilde{a}_{2;3}(\mathbf{q}; \omega)$  for the  $Q_2$  or  $Q_3$  modes. The amplitude response function is given by,

$$\tilde{a}_{2;3}(\mathbf{q}; \omega) = \sum_{\mathbf{k}, \mathbf{k}^0}^X f(\mathbf{k} + \mathbf{q}; \mathbf{k}^0 + \mathbf{q})$$

$$\text{hh} \left( \sum_{i=1,2}^X \frac{y_{ik}(t) \wedge_{1-ik+q}(t)}{y_{ik^0+q}(0) \wedge_{1-ik^0}(0)} \right) \text{ii} \downarrow; \quad (21)$$

where

$$\begin{aligned} f(k; k^0) &= \sin_k \sin_{k^0}; \quad \text{for } Q_2 \text{ mode} \\ &= \cos_k \cos_{k^0}; \quad \text{for } Q_3 \text{ mode}; \end{aligned} \quad (22)$$

and  $\frac{y_{1,2;2}}{y_{1,2;2} k} (C_k^{1,2} y_{C_{k+Q}^{2,1} y})$ , are similar to Nam bu operators.  $\wedge_1$  is the Pauli matrix.

Within the random phase approximation (RPA), we obtain,

$$\frac{a_{2,3}^a(q; \frac{\omega}{\hbar})}{1 - g_{2,3}^a(q; \frac{\omega}{\hbar})} = \frac{a_{2,3}^a(q; \frac{\omega}{\hbar})}{1 - g_{2,3}^a(q; \frac{\omega}{\hbar})}; \quad (23)$$

The spectral density function is related to imaginary part of  $\text{RPA}(\frac{\omega}{\hbar})$ , which is given by,

$$S(0; \frac{\omega}{\hbar}) = \text{Im} \frac{a_{2,3}^a(q; \frac{\omega}{\hbar})}{(1 - g_{2,3}^R(0; \frac{\omega}{\hbar}))^2 + (g_{2,3}^I(0; \frac{\omega}{\hbar}))^2}; \quad (24)$$

where  $g_{2,3}^R(0; \frac{\omega}{\hbar})$  and  $g_{2,3}^I(0; \frac{\omega}{\hbar})$  are respectively the real and imaginary part of  $a_{2,3}^a(0; \frac{\omega}{\hbar})$ . By using equation (21) the expressions for  $a_{2,3}^a(0; \frac{\omega}{\hbar})$  are obtained as,

$$\begin{aligned} a_2^a(0; \frac{\omega}{\hbar}) &= 4 \sin^2_k (Q; \frac{\omega}{\hbar}) \\ a_3^a(0; \frac{\omega}{\hbar}) &= 4 \cos^2_k (Q; \frac{\omega}{\hbar}); \end{aligned} \quad (25)$$

with

$$(Q; \frac{\omega}{\hbar}) = \sum_k^X \cos^2_k \frac{E_k^1 \tanh(E_k^1 = 2)}{\frac{\omega^2}{4E_k^1} + \cos^2_k \frac{E_k^2 \tanh(E_k^2 = 2)}{\frac{\omega^2}{4E_k^2}}}; \quad (26)$$

### 3. Results and Discussions

In previous section we have formulated a theory for the charge density wave state in a Jahn-Teller active system. Self consistent solution of equation (17) or (18) yields  $\omega_2$

or  $\epsilon_3$  respectively. All parameters are expressed in units of  $t$  however temperature  $T$  is expressed as  $T = k_B T t$ . In Fig. 1, we show the variation of  $\epsilon_2$  and  $\epsilon_3$  (in units of  $t$ ) with temperature  $T$  in a FM spin state. It is evident that the magnitude of JTCCDW gap decreases with increasing temperature. The magnitude as well as transition temperature  $T_{\text{CDW}}$  for  $Q_3$  mode is larger than that of  $Q_2$  mode for  $g = 1$ . The magnitude of  $\epsilon_3$  is not always larger than  $\epsilon_2$ . This is depicted in Fig. 2, where variation of JTCCDW gap with  $g$  is shown for a very low temperature. It is shown in Fig. 2 that  $Q_2$  distortion mode opens up JTCCDW gap at a lower value of  $g$  than that due to  $Q_3$  mode and  $\epsilon_3$  is less than  $\epsilon_2$  till  $g = 0.6$ . With increasing value of  $g$  both  $\epsilon_2$  and  $\epsilon_3$  increases and for values of  $g$  greater than 0.6,  $\epsilon_2$  is less than  $\epsilon_3$ . So it is clear that the JT modes have different electron-phonon interaction dependences.

To determine the dominant JT mode we show the variation of free energy  $F$  in FM state, with  $g$  in Fig. 3. At very small values of  $g$ , eph coupling does not alter the energy significantly, hence presence of either of the JT modes yield the same energy. For higher values of  $g$  the JT coupling becomes pronounced and it is evident from Fig. 3 that  $Q_2$  distortion mode acquires lowest free energy for any value of  $g$ . In Fig. 4 the variation of free energy for AFM spin state is shown, which is taken into account through double exchange interaction. In AFM spin arrangement also  $Q_2$  mode yields lower energy than  $Q_3$  mode while the respective energy values are much higher than those in FM ordering. It can be shown that the  $g$  dependence of  $\epsilon_2$  and  $\epsilon_3$  in AFM ordering are similar as FM case. The obtained ground state of our two dimensional model, with one electron per site, is in agreement with the undoped LaMnO<sub>3</sub> where spins are arranged in FM order in x-y plane.

It is well known that low temperature heat capacity ( $C_V$ ) of CMR manganites has a bearing on many fundamental properties like density of states, lattice contribution and spin wave stiffness. Recent experiments on insulating LaMnO<sub>3</sub> [20] show that at low temperature,  $C_V = T$  vs  $T^2$  plot gives approximately straight lines. In an earlier

work [21], we have shown that in a two-site, single orbital, double exchange model the lattice contribution is dominant in FM configuration as far as core spins are of quantum nature. However, in the present work, due to inclusion of orbital degeneracy it is expected that JT phonons will show dominance. In an attempt to compare the lattice contributions of the specific heat in JT CCDW state driven by  $Q_2$  or  $Q_3$  mode, we show the thermal variations of the heat capacity  $C_V$  at low temperature in Fig. 5 and a plot of  $C_V = T$  vs  $T^2$  in Fig. 6. It is clear from Fig. 5 that nature of variation of specific heat of the system for any of the JT modes are similar at low temperature. Fig. 6 shows that at low temperature the  $T^3$  behavior is pronounced for both the JT modes but the Debye temperatures seem to be different.

Very recently in Raman scattering experiment on LaMnO<sub>3</sub> [22] by Saitoh et al, the orbital excitations were observed. According to Brink [23], the elementary excitations of LaMnO<sub>3</sub> show both the orbital and phonon character due to the mixing of orbital and phonon modes. In the present system, JT CCDW state occurs due to softening of either  $Q_2$  mode or  $Q_3$  mode. Here charge densities at different  $e_g$  orbitals depend on whether  $Q_2$  or  $Q_3$  phonon coupling is active. The  $Q_3$  mode couples with the electron density difference of  $d_{x^2-y^2}$  and  $d_{3z^2-r^2}$  orbitals whereas the  $Q_2$  mode interacts with the charge density difference between bonding and anti-bonding orbitals formed by these two orbitals [14]. It is expected that the low lying collective excitations of resulting JT CCDW will show different  $g$  dependence for  $Q_2$  and  $Q_3$  modes. It is evident from equation (24), (25) and (26) that spectral density function  $S(0;\epsilon)$  for amplitude mode at some symmetry points are due to any one of the JT modes. As example, all spectral density at symmetry point (0, 0) is due to  $Q_3$  mode while at (1, 0) only  $Q_2$  mode contributes to  $S(0;\epsilon)$ . It is also obvious that at these symmetry points the CDW gap exists due to the JT mode which contributes to  $S(0;\epsilon)$ . However, the  $S(0;\epsilon)$  as well as  $\chi$  at (1, 0) = 2) is finite for both  $Q_2$  and  $Q_3$  mode. In Fig. 7 and Fig. 8 we show  $S(0;\epsilon)$  at (1, 0) = 2) for different values of  $g$  in  $Q_2$  and  $Q_3$  excited CDW

state respectively. With increasing  $g$  the peak shifts to higher values of frequency  $\omega$  for both the JT modes, because the amplitude of the JT CCDW gap increases for both the modes. It is important to note that the peak position of  $S(0; \omega)$  shifts more for  $Q_2$  mode than that of  $Q_3$  with equal increase of  $g$ . So the electron-lattice interaction has more pronounced effect on the collective excitations of  $Q_2$  active CDW state than that of  $Q_3$  mode.

The present calculation is done for a half-filled system when any one of the JT modes is active. In real systems both the modes may be excited simultaneously. It is expected that in that case  $Q_2$  mode will be the dominating one. With hole doping in the half-filled system there will be decrease of Jahn-Teller active  $Mn^{3+}$  ions and the perfect nesting of the Fermi surface will be destroyed. These are expected to reduce the effective electron-JT interaction as well as JT CCDW gap  $\omega_k$ , which may yield an orbitally disordered system. The work along these lines are in progress.

#### 4. Conclusions

The charge density wave may have its origin due to softening of the breathing mode phonon or Jahn-Teller phonons. Emergence of the Jahn-Teller coupled charge density wave is relevant in a system where Jahn-Teller phonons play a crucial role to determine the orbital ordering. In the limit of one electron per site and strong Hund's rule coupling, we provide a comprehensive study of the formation of charge density wave emphasizing on  $e_g$  electron - Jahn-Teller coupling in a orbital ordered system with two kinds of orbitals alternating on adjacent sites in the  $x-y$  plane. The in-plane distortion mode  $\{Q_2\}$  is the dominant mode and it opens up JT CCDW gap at smaller electron-lattice interaction strength than the octahedral stretching mode  $\{Q_3\}$ . The heat capacity shows  $T^3$  behavior at low temperature which are in quali-

tative agreement with experimental findings [20]. At some of the  $k$ -points, the effect of the electron-lattice interaction on collective mode such as amplitude mode is more pronounced when the excited Jahn-Teller mode is  $Q_2$ .

I acknowledge many useful discussions with Prof. S. Yarlagadda.

## REFERENCES

[1] For a review, Y. Tokura, Ed., *Colossal Magnetoresistive Oxides*, (Gordon and Breach, New York, 2000).

[2] Y. Murakami, J. P. Hill, D. G. Gibbs, M. Blume, I. Koyama, M. Tanaka, H. Kawata, T. Arima, Y. Tokura, K. Hirota and Y. Endoh, *Phys. Rev. Lett.*, 81, 582 (1998).

[3] T. Nagai, T. Kimura, A. Yamazaki, K. Kimoto, Y. Yokura and Y. Matsui, *Phys. Rev. B* 68, 092405 (2003).

[4] Noriaki Kida and Masayoshi Tonouchi, *Phys. Rev. B* 66, 024401 (2002).

[5] Y.-D. Chuang, A. D. Gromko, D. S. Dossau, T. K. Kimura, Y. Tokura, *Science* 292, 1509 (2001).

[6] A. Wahl, S. M. Ercoone, A. Pautrat, M. Pollet, Ch. Simon and D. Sedmidubsky, *Phys. Rev. B* 68, 094429 (2003).

[7] D. N. Argyriou, H. N. Bordallo, B. J. Campbell, A. K. Cheetham, D. E. Cox, J. S. Gardner, K. Hanif, A. dos Santos, G. F. Strouse, *Phys. Rev. B* 61, 15269 (2000).

[8] B. J. Campbell, R. O. Stommel, D. N. Argirou, L. Vasiliu-Doloc, J. F. M. Mitchell, S. K. Sinha, U. Ruett, C. D. Ling, Z. Islam and J. W. Lynn, *Phys. Rev. B* 65, 014427 (2002).

[9] G. Gruner, *Rev. Mod. Phys.* 60, 1129 (1988).

[10] Phillip B. Allen and Vasili Perebeinos, *Phys. Rev. B* 60, 10747 (1999).

[11] P. W. Anderson and H. Hasegawa, *Phys. Rev.* 100, 675 (1955).

[12] G. D. Mahan, *Many Particle Physics*, (Plenum Press, New York, 1981).

[13] Sudhakar Yarlagadda, *Int. Jr. Mod. Phys.*, 27, 3529 (2001).

[14] Sudhakar Yarlagadda and Manidipa Mitra, cond-mat/0310350.

[15] C. K. Kittel, *Quantum Theory of Solids*, (John Wiley and Sons, Inc., New York, 1987).

[16] G. Jackeli, N. B. Perkins and N. M. Plakida, *Phys. Rev. B* 62, 372 (2000).

[17] R. Maezono, S. Ishihara and N. Nagaoza, *Phys. Rev. B* 57, R13 993 (1998).

[18] L. F. Feiner and A. M. Oles, *Phys. Rev. B* 59, 3295 (1999).

[19] T. Hotta, S. Yunoki, M. M. Mays and E. Dagotto, *Phys. Rev. B* 60, R15 009 (1999).

[20] L. G. M. Huijvelde, I. Abrego Castillo, M. A. Gusev, J. A. Alonso, L. F. Cohen, *Phys. Rev. B* 60, 12184 (1999).

[21] M. Anidipa Mitra, P. A. Sreeram and Sushanta Datta Gupta, *Phys. Rev. B* 67, 132406 (2003).

[22] E. Saitoh, S. Okamoto, K. T. Takahashi, K. Kubo, K. Yamamoto, T. Kimura, S. Ishihara, S. Maekawa and Y. Tokura, *Nature (London)* 410, 180 (2001).

[23] Jeroen van den Brink, *Phys. Rev. Lett.* 87, 217202 (2001).

Figure captions :

Fig. 1. Thermal variations of the  $\epsilon_2$  (solid line) and  $\epsilon_3$  (dashed line) in FM state, for  $g = 1.0$ .

Here,  $\tilde{T} = k_B T t$ .

Fig. 2. Variations of  $\epsilon_2$  (solid line) and  $\epsilon_3$  (dashed line) with  $g$  at  $\tilde{T} = (k_B T t) = 10^5$  in FM state.

Fig. 3. Variation of free energy  $F$  in FM state for  $Q_2$  distorted CDW state (solid line) and  $Q_3$  distorted CDW state (dashed line) with  $g$  at  $\tilde{T} = 0.005$ .

Fig. 4. Variation of free energy  $F$  in AFM state for  $Q_2$  distorted CDW state (solid line) and  $Q_3$  distorted CDW state (dashed line) with  $g$  at  $\tilde{T} = 0.005$ .

Fig. 5. Variation of  $C_V$  (in arbitrary units) with  $\tilde{T}$  for  $Q_2$  active (solid line) and  $Q_3$  active (dashed line) CDW state for  $g = 1.0$  in FM state.

Fig. 6.  $C_V = \tilde{T}$  vs  $\tilde{T}^2$  plot in FM state for  $Q_2$  active (solid line) and  $Q_3$  active (dashed line) CDW state with  $g = 1.0$ . Here  $C_V$  is in arbitrary units and  $\tilde{T} = k_B T t$ .

Fig. 7. Spectral density functions  $S(0; \omega)$ , for the JT CCDW amplitude mode as a function of frequency  $\omega$  (in unit of  $t$ ) in presence of  $Q_2$  distortion, at k-point ( $\Gamma, \Gamma$ ), for different values of  $g = 0.45, 1.0, 1.5$ .

Fig. 8. Spectral density functions  $S(0; \omega)$ , for the JT CCDW amplitude mode as a function of frequency  $\omega$  (in unit of  $t$ ) in presence of  $Q_3$  distortion, at k-point ( $\Gamma, \Gamma$ ), for different values of  $g = 0.45, 1.0, 1.5$ .

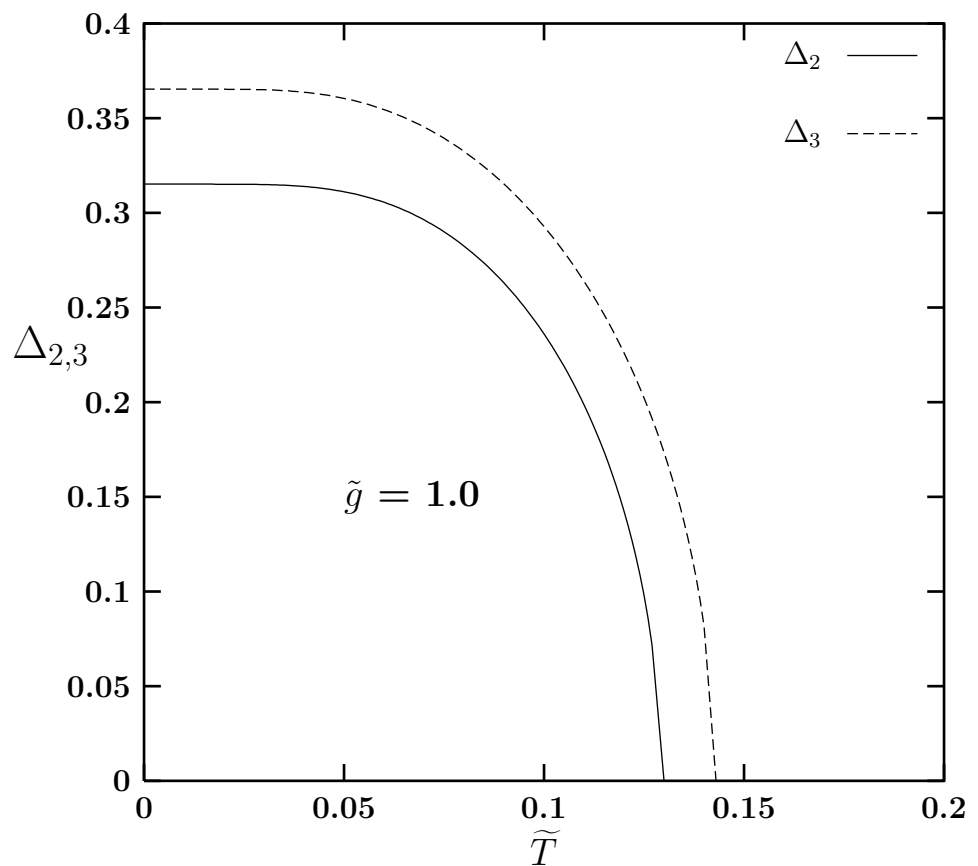


FIG. 1

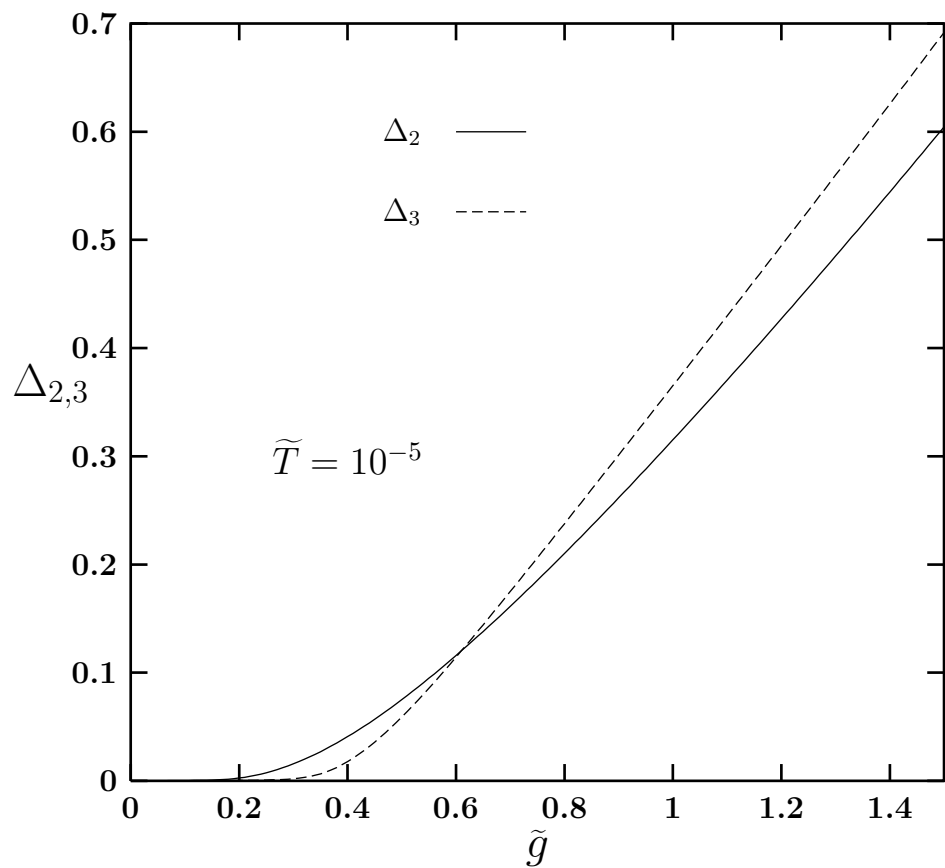


FIG. 2

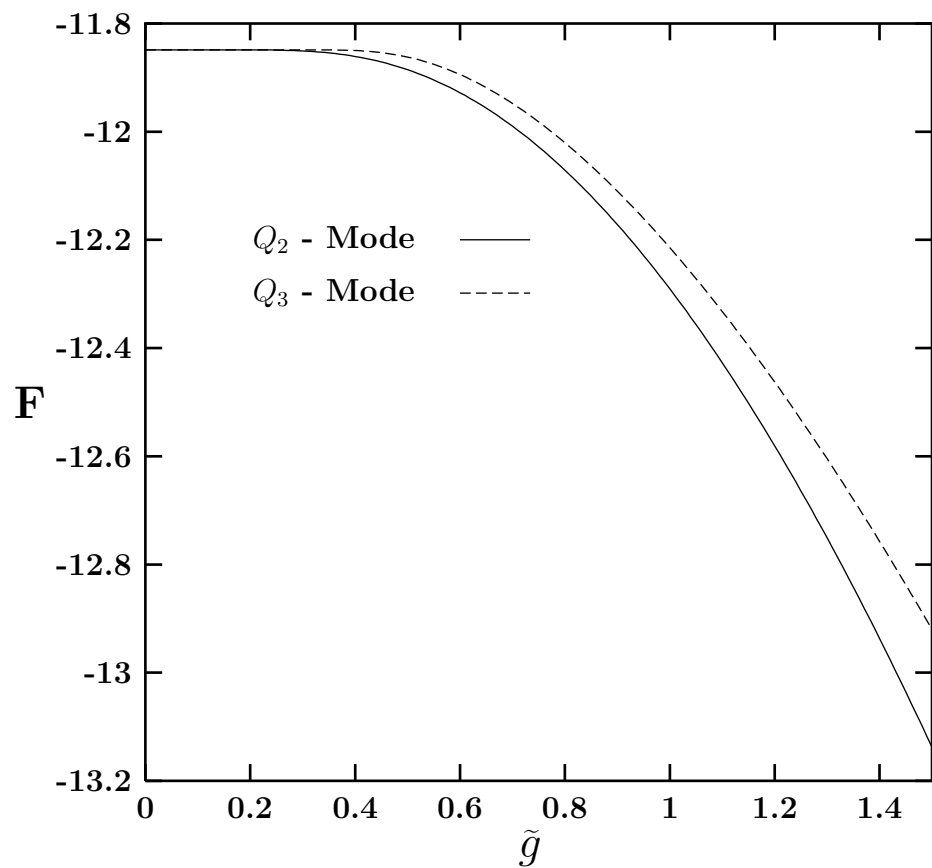


FIG. 3

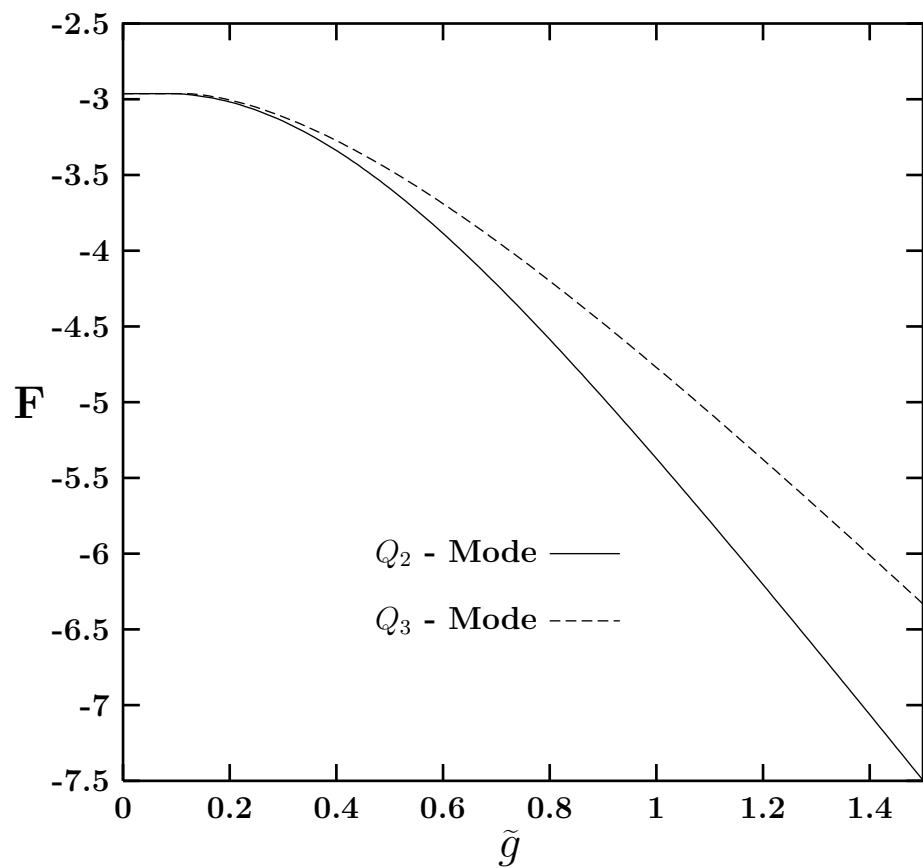


FIG. 4

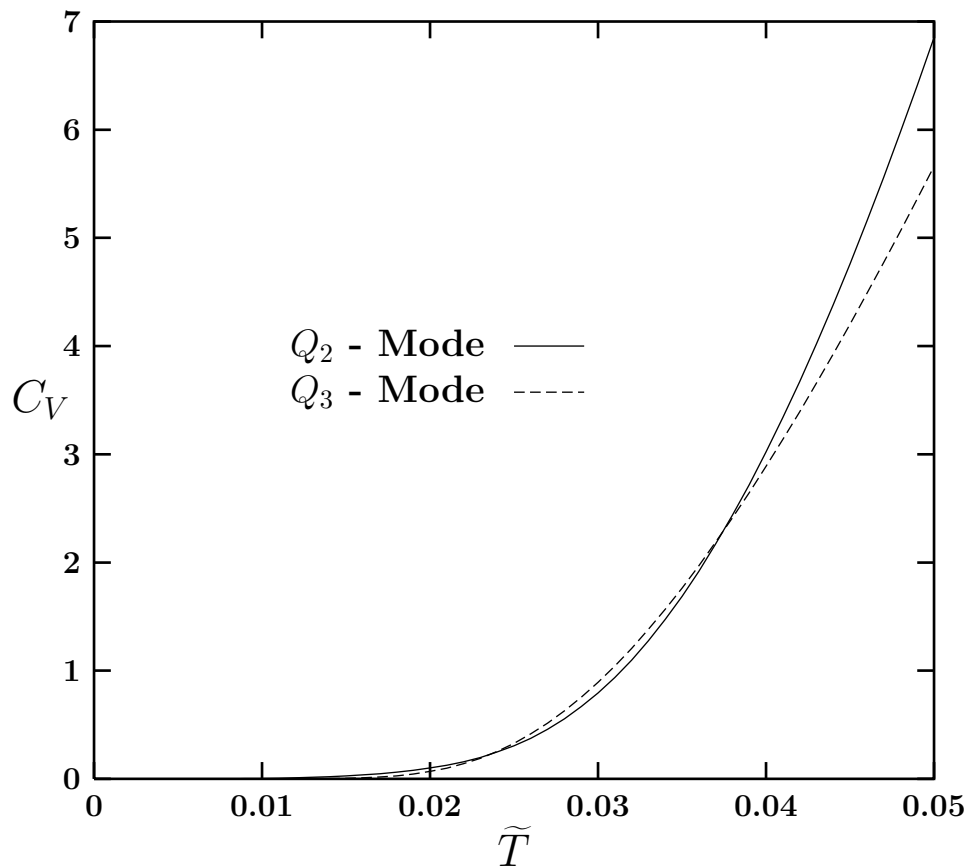


FIG. 5

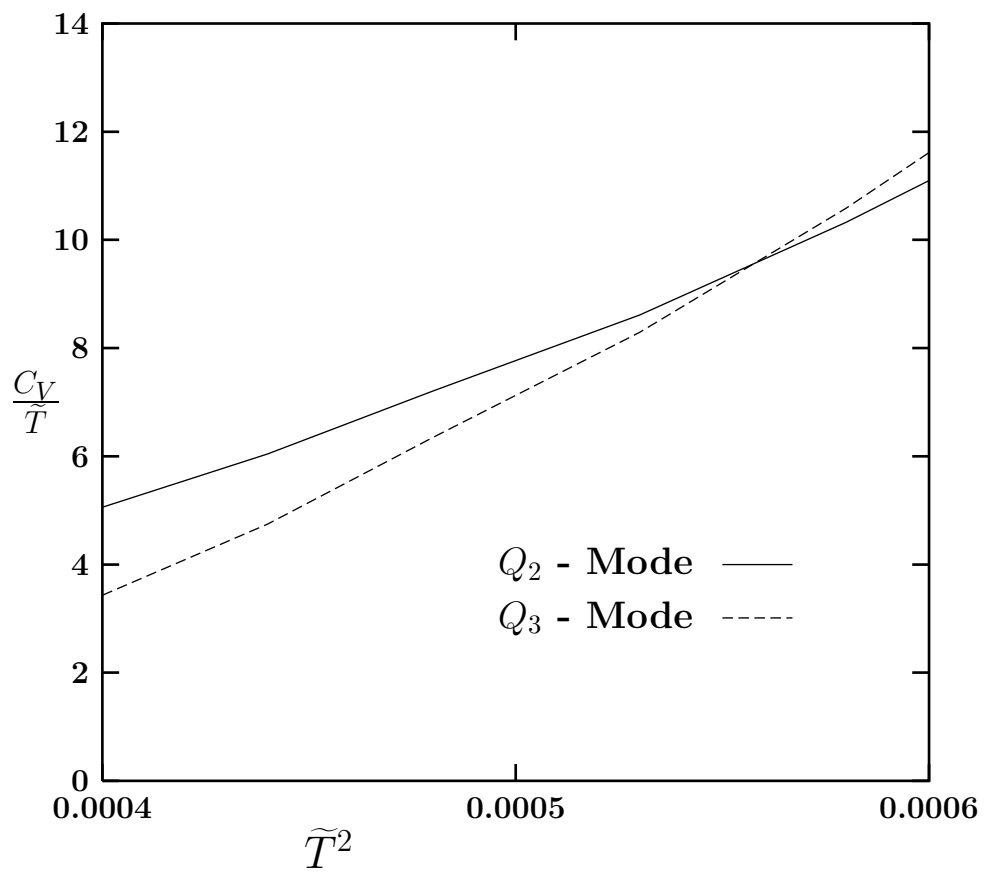


FIG. 6

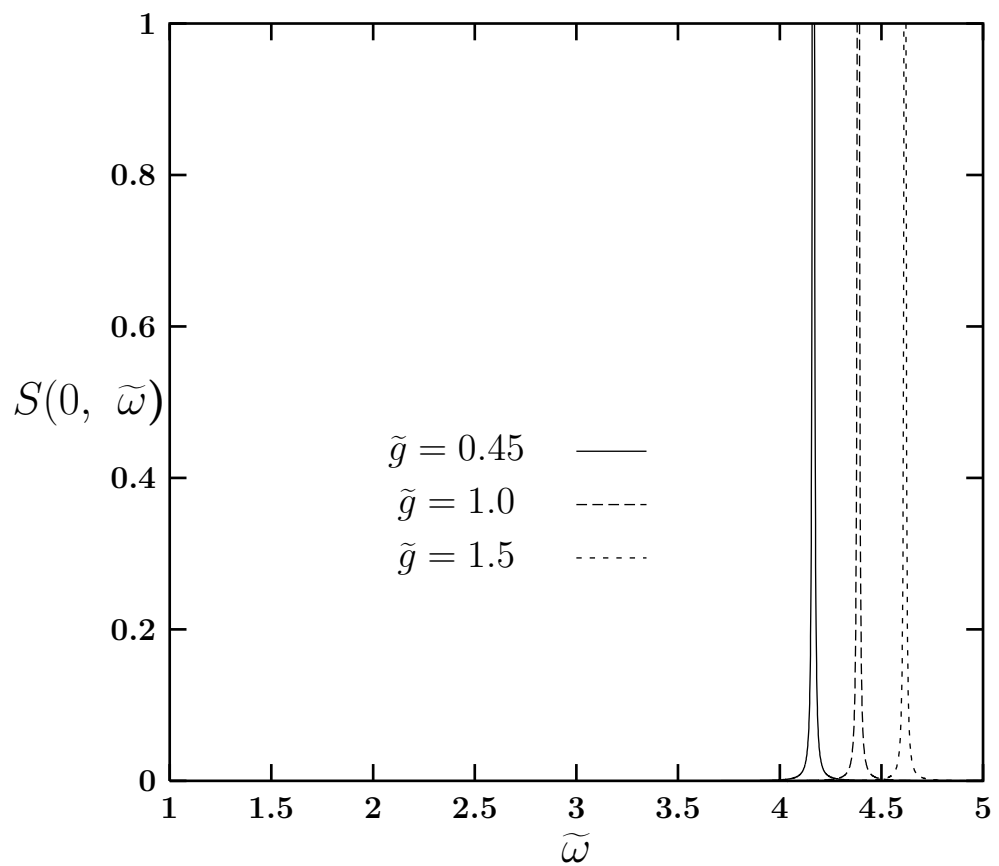


FIG. 7

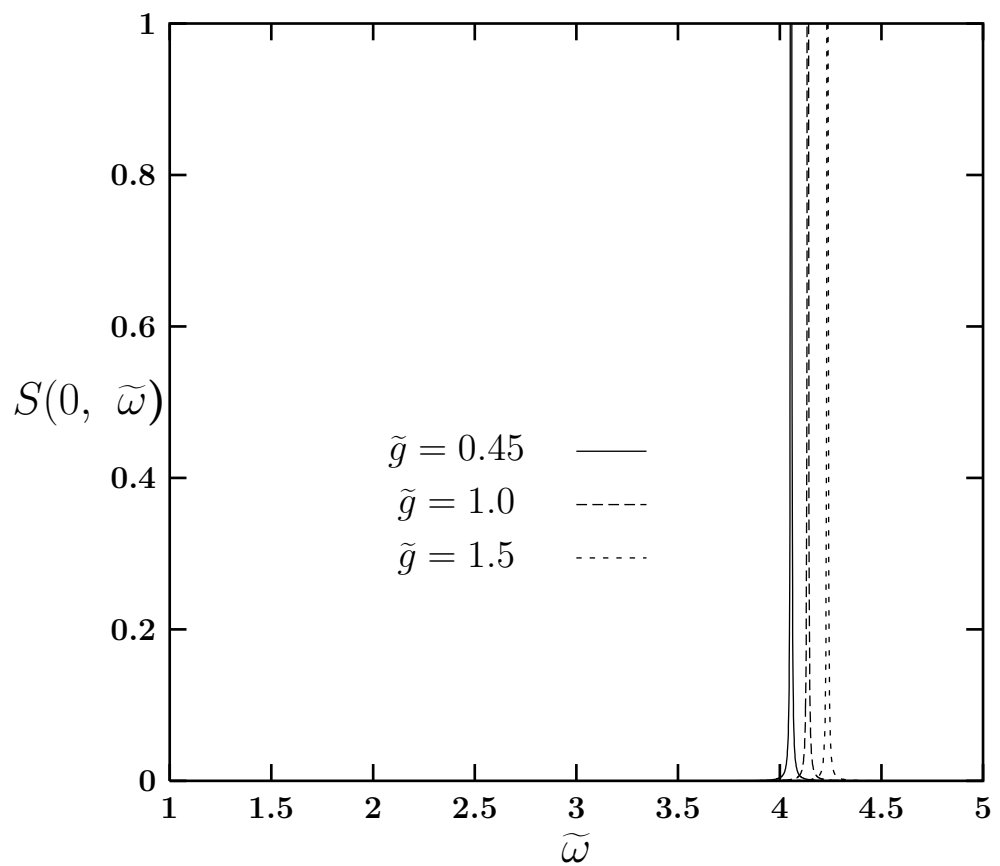


FIG. 8